The Journal of Physiology

Title: Regional activation in the human longissimus thoracis pars lumborum muscle

Authors: Jacques Abboud
Calvin Kuo
Martin Descarreaux
Jean-Sébastien Blouin

Author Conflict: No competing interests declared

Author Contribution: Jacques Abboud: Conception or design of the work; Acquisition or analysis or interpretation of data for the work; Drafting the work or revising it critically for important intellectual content; Final approval of the version to be published; Agreement to be accountable for all aspects of the work Calvin Kuo: Acquisition or analysis or interpretation of data for the work; Drafting the work or revising it critically for important intellectual content; Final approval of the version to be published; Agreement to be accountable for all aspects of the work Martin Descarreaux: Conception or design of the work; Drafting the work or revising it critically for important intellectual content; Final approval of the version to be published; Agreement to be accountable for all aspects of the work Jean-Sébastien Blouin: Conception or design of the work; Acquisition or analysis or interpretation of data for the work; Drafting the work or revising it critically for important intellectual content; Final approval of the version to be published; Agreement to be accountable for all aspects of the work

Running Title: Longissimus motor units organization

Disclaimer: This is a confidential document.

Dual Publication: No

Regional activation in the human longissimus thoracis pars lumborum muscle

Jacques Abboud[1,2], Calvin Kuo[2], Martin Descarreaux[1], Jean-Sébastien Blouin[2]

[1] *Département des Sciences de l'Activité Physique, Université du Québec à Trois-Rivières, Trois-Rivières, Canada*

[2] *School of Kinesiology, University of British Columbia, Vancouver, Canada*

Corresponding author

Jean-Sébastien Blouin

Address: 210–6081 University Blvd, Vancouver, BC, V6T1Z1 Canada

Telephone: 604 827–3372

Email: jsblouin@mail.ubc.ca

Running title: Longissimus motor units organization

Key points

- Longissimus activity in the lumbar region was measured using indwelling electromyography to characterize the territory of its motor units.

- The distribution of motor units in the longissimus pars lumborum muscle was mainly grouped into two distinct regions.

- Regional activation of the longissimus pars lumborum was also observed during functional tasks involving trunk movements.

- The regional activation of the longissimus pars lumborum muscle may play a role in segmental stabilization of the lumbar spine.

Abstract

The longissimus pars lumborum contributes to lumbar postural control and movement. While animal studies suggest a segmental control of this muscle, the territory of motor units constituting the human longissimus pars lumborum remains unknown. The aims of this study were to identify the localization of motor unit territories in the longissimus and assess the activation of this muscle during functional tasks. Eight healthy participants were recruited. During isometric back extension contractions, single motor-unit (at L1, L2, L3 and L4) and multi-unit indwelling recordings (at L1, L1-L2, L2, L2-L3, L3, L3-L4 and L4) were used to estimate motor unit territories in the longissimus pars lumborum based on the motor-unit spike-triggered averages from fine-wire electrodes. A series of functional tasks involving trunk and arm movements were also performed. A total of 73 distinct motor units were identified along the length of the longissimus: only two motor units spanned all recording sites. The majority of the recorded motor units had muscle fibers located in two main rostro-caudal territories (32 motor units spanned L1 to L3 and 30 spanned ~L3 to L4) and 11 had muscle fibers outside these two main territories. We also observed distinct muscle activation between the rostral and caudal regions of the longissimus pars lumborum during a trunk rotation task. Our results show clear rostral and caudal motor unit territories in the longissimus pars lumborum muscle and suggest that the central nervous system can selectively activate regions of the superficial lumbar muscles to provide local stabilization of the spine.

Keywords: Erector spinae; lumbar spine; electromyography; motor unit

INTRODUCTION

The trunk is a complex anatomical system with many muscles acting synergistically to maintain posture and generate movement. In the lumbar region, the erector spinae - comprised of the iliocostalis, longissimus and spinalis muscles - contribute to lumbar postural control and movement (Bergmark, 1989; Moseley *et al.*, 2002). Activation of these muscles suggests they act as a single unit to exert forces and moments on the spine, with no evidence they can contribute to stabilization of individual lumbar segments (Moseley *et al.*, 2002). The human longissimus thoracis pars lumborum muscle (abbreviated thereafter as longissimus pars lumborum), however, possesses distinct heads originating from the lumbar vertebrae (mammillary, accessory and transverse processes) that insert on the caudal part of the posterior sacrum and the medial edge of the iliac crest (Kalimo *et al.*, 1989; Christophy *et al.*, 2012) (Figure 1A). Its L1 to L4 fascicles are composed of muscular and musculotendinous fibres that form the lumbar intermuscular aponeurosis with fibers from rostral segments covering those from caudal ones (Macintosh & Bogduk, 1987). Consequently, muscles fibres comprising the longissimus pars lumborum have different lengths depending on the vertebral level they originate from and the level at which they insert onto the lumbar intermuscular aponeurosis. Further, the orientation of the erector spinae muscle fibers vary across lumbar segments between different functional tasks (Harriss & Brown, 2015). In cats, synaptic connections to the longissimus pars lumborum motoneurones are partly organized to enhance segmental control of the lumbar spine (Wada *et al.*, 2003; Durbaba *et al.*, 2007). Specifically, group I muscle spindle afferents from the cat longissimus pars lumborum muscle project to the same segment and to one or two adjacent segments, while group II muscle afferents are widely distributed along lumbar segments (Wada *et al.*, 2003). These anatomical and physiological observations from human and cat studies raise the possibility that the human longissimus pars lumborum may be activated segmentally, likely via the organization of its motor unit (MU) territories based on the origin of its muscle fibers onto distinct lumbar vertebral levels.

Regional activation of human muscles has been proposed as a way to allow for more controlled and efficient torque generation (Butler, 2007; Hudson *et al.*, 2009; Wakeling,

2009). Such regional activation has been described for axial muscles in humans: the caudal regions from the longissimus thoracis exhibit differential activations from rostral regions during ipsilateral trunk rotation (Lee *et al.*, 2005). The longissimus pars lumborum is innervated segmentally with multiple end plates, also allowing for potential segmental control through the activation of MUs innervating muscles fibers in defined lumbar regions (Bogduk *et al.*, 1982; Bogduk, 1983). The multi-layered architecture and angle of the longissimus pars lumborum muscle fibers with respect to the skin, however, renders the detection of MU action potential propagation along their muscle fibers difficult with surface electromyography (Shiraishi *et al.*, 1995; Beretta Piccoli *et al.*, 2014). These challenges highlight the need to use intramuscular recordings to assess the distribution of longissimus pars lumborum muscle fibers innervated by individual motoneurons. The estimation of human MU territories using a combination of single MU and multi-unit indwelling recordings revealed broad distribution of muscle fibers comprising a MU in the medial gastrocnemius (Héroux *et al.*, 2015), challenging the presence of regional MU territories in this muscle.

Our understanding of MU physiology in the human longissimus thoracis (pars thoracis and lumborum) is limited, with no information available regarding the organization and distribution of its MUs. In the present experiment, our main objective was to characterize the territory of the human longissimus pars lumborum MUs. In particular, we used the technique developed by Harris *et al.* (2005) to estimate the size (i.e. electrophysiological rostro-caudal territory occupied by the muscle fibers innervated by a single motoneuron) and organization of MU territories in the longissimus pars lumborum. Based on its anatomy, segmental innervation and physiological observations in the cat (Wada *et al.*, 2003; Durbaba *et al.*, 2007), we hypothesized that longissimus pars lumborum muscle fibers belonging to a given MU would be spatially localized rather than being uniformly distributed along the entire length of the muscle. As a secondary objective, we assessed if regional activation of the longissimus pars lumborum was physiologically relevant during functional trunk and arm movements.

METHODS

Participants

Eight healthy adult volunteers (seven males and one female) with no history of acute/chronic thoracic or low back pain in the past 6 months, sensorimotor dysfunction, trunk neuromuscular disease, inflammatory arthritis, and previous spinal surgery participated in this study. Participant mean (*M*) age, height, weight and BMI were respectively 28.9 (standard deviation (*SD*) = 6.6) years, $M = 1.75$ ($SD = 0.1$) m, $M = 72.5$ ($SD = 12.5$) kg and $M = 23.7$ ($SD = 3.1$) kg/m^2. The study conformed to the *Declaration of Helsinki*, except for registration in a database, and was approved by the University of British Columbia's Clinical Research Ethics Board (H16-01636). All participants gave written informed consent, acknowledging their right to withdraw from the experiment without prejudice.

Multi-unit fine-wire recordings

Prior to the insertion of the fine-wire electrode, we measured the height and weight of the participants. We identified the longitudinal and medio-lateral limits of the left longissimus pars lumborum muscle using ultrasound (SonoSite Micro Maxx, Bothell, WA, USA) and marked them on the participants' skin. We also took four ultrasound pictures per participant, one at each level (L1, L2, L3 and L4) in order to estimate the orientation of the muscle fibers. Prior to the insertion of the fine-wire electrodes, the skin was cleaned thoroughly with alcohol. Intramuscular multi-unit EMG bipolar signals were recorded with fine-wire electrodes custom-made from two 0.05mm insulated stainless steel wires (California Fine Wire, Grover Beach, CA, USA). The distal parts of the wires were bent to create two barbs of 3-4mm and 10mm length. We removed the distal 5mm of insulation from the longer barb to favour multi-units recordings. The pairs of wires were wound together and inserted via a 1.5 inch 25 gauge hypodermic needle (EXEL International Medical Products, St Petersburg, FL, USA). All needles and wires were used once and sterilized using a medical grade sterilizer (PVdry2 Barnstead-Harvey, Dubuque, IA, USA) prior to use. A surface electrode (Ag/AgCl surface electrode, Ambu Blue, SensorM,

Ballerup, Denmark) was placed over the posterior superior iliac spine on the left side and served as the ground for fine-wire electrode recordings.

To determine the rostro-caudal distribution of the longissimus MUs, we inserted fine-wire electrodes in the left longissimus pars lumborum at 7 different sites (L1, L1-L2, L2, L2-L3, L3, L3-L4 and L4) with 10-15mm inter-electrode spacing. The most caudal part of the longissimus pars lumborum (L4-L5 and L5 segments) was not considered in this study because it was too difficult to discriminate the longissimus pars lumborum from other lumbar muscles at these levels using ultrasound. The insertions were performed under ultrasound guidance. The fine-wires were inserted in the longissimus with an angle of ~ 35 degrees with a lateral to medial direction at a target depth of ~ 2 cm (Figure 1B). This insertion method ensured that the recording site was located within a small region perpendicular to the longissimus muscle rostro-caudal axis and that the exposed wire did not overlap between recording sites. The needles were inserted ~ 3 cm (range 2.5-3.3) laterally from the spinous process at L1 and ~ 3.5 cm (range 3.1-3.9) at L4.

[Figure 1]

Single-unit microelectrode recordings
One tungsten needle was used to record single MU activity (0.2 mm diameter, 45 mm length, standard profile tip, Fred Haer Inc., Bowdoin, MA, USA). A second uninsulated tungsten microelectrode (0.2 mm diameter, 45 mm length, standard profile tip, Fred Haer Inc., Bowdoin, MA, USA) was inserted under the skin over the iliac crest and served as the reference. All microelectrodes were sterilized similarly to the multi-unit electrodes prior to use.
Fine-wire and microelectrode signals were filtered (band-pass 30–3000 Hz) and amplified (×500–1000, NeuroLog System NL844 & NL820, Digitimer, Welwyn Garden City, UK). EMG data were sampled at 10 kHz (fine-wire) and 30 kHz (microelectrode) with a 16-bit CED DAQ and Spike2 software (Cambridge Electronics Design, Cambridge, UK).

Experiment 1: Motor unit territory protocol

After the insertion of the fine-wire electrodes, participants were asked to perform weak isometric back extension muscle contractions against a force plate (AMTI model OR6-7-1000, Watertown, MA, USA) contacting the thoracic region while prone on a table. Force plate signals were sampled at 500 Hz using the 16-bit CED DAQ and Spike2 software (Cambridge Electronics Design, Cambridge, UK). The height of the force plate was adjusted for each participant so that small forces from weak back extension contractions could be recorded. Then, the tungsten microelectrode electrode was inserted near one of four fine-wire recording sites in the longissimus pars lumborum muscle: L1, L2, L3 and L4. The insertions of the microelectrode were performed perpendicular to the skin directly above the location of the tip of the fine-wire electrodes at one of these four sites.

Participants performed a series of weak voluntary back extension contractions, gradually increasing the intensity until a MU could be identified and recorded. Once a target contraction intensity allowing us to identify a single MU was reached, participants were asked to hold this contraction as steady as possible during 90-120 s. Based on reported lumbar muscles MUs firing rate (~ 6 pulses/s (Marsden *et al.*, 1999; Lothe *et al.*, 2015)), we estimated that ~500 MUs should be recorded per trial during this time. Verbal feedback from the experimenters as well as auditory feedback provided by the MU discharge rate helped participants hold a steady contraction and consistent MU firing during the isometric contractions. Once a trial was completed, participants were asked to perform additional voluntary contractions at a higher intensity in order to recruit new MUs. This protocol was repeated until it was no longer possible to record and isolate newly recruited MUs. Between contractions, the tungsten electrode was slightly moved within the same site to increase the possibility to record a different MU. Four to eight contractions were performed per participants at each of the recording site (L1, L2, L3 and L4) within the longissimus pars lumborum muscle. The tungsten electrode was then moved to a different site near the location of another fine-wire recording sites to record single MU action potentials around that site. Between each new tungsten electrode insertion and/or at the participant's request, a rest period up to 5 minutes was provided to avoid back muscle fatigue.

To determine the percentage of maximal voluntary isometric contraction (MVC) at which the contractions were performed and to normalize the multi-unit EMG activity recorded during the functional task protocol (see below), MVCs were performed at the end of the MU protocol. Participants performed three to five back isometric extension MVCs while in the same position as during the MU protocol. For each MVC, participants were asked to push as hard as possible against the force plate for 3-5 seconds. The fourth and fifth MVC trials were only performed if the participant's third MVC was superior to the first and second one. A one-minute rest period was provided between trials and verbal encouragements were provided by the experimenters. None of the participants reported pain during the MVC protocol. Around 75% of back extensions performed during the single MU recordings ranged between 1 and 10% of their MVC, while 20% ranged between 10 and 20% and 5% higher than 20% of MVC (21-42%).

Experiment 2: Functional task protocol

Following the MU protocol, participants were asked to perform functional tasks to assess if the regional activation single MU had any physiological relevance. We asked participants to perform [A] Shoulder flexion, [B] Trunk rotation, and [C] Slouched sitting tasks to replicate everyday life arm/trunk movements and because these tasks modify the orientation of the lumbar erector spinae muscle fibers. The timing of the movements was controlled by an auditory metronome to standardize each task. [A] Shoulder Flexion. In a neutral upright posture with their arms along their sides, participants were asked to perform a flexion of their left shoulder until they reached their full range of motion (~180 degres) in 5 seconds. Participants were asked to hold this position for 3 to 5 seconds and to go back to their initial position in 5 seconds. [B] Trunk rotation. In a neutral seated posture, participants performed a trunk axial rotation. They iniated the movement in a neutral posture, then rotated the trunk to one side in 5 seconds and returned to their intial posture in 5 seconds. The same procedure was performed for trunk rotation to their other side. Participants were asked to rotate their trunk at their maximal range of motion without creating pelvis rotation. [C] Slouched sitting. In a neutral seated posture, participants were asked to adopt a slouched sitting posture for up to 10 seconds and returned to their initial

posture. Finally, we also tried to record muscle activity during trunk flexion. This task, however, was not considered for the analysis because only one participant was able to perform the task without experiencing lumbar pain.

During the functional tasks, myoelectric activity of the longissimus pars lumborum muscle was recorded from the multi-unit EMG recordings as above. Trunk and left arm kinematics were also recorded using two digital video cameras (Fujifilm FinePix JX600 and Sony DSC-RX100M5). One camera was positioned on a tripod located approximately 3 meters from the participants in order to record trunk kinematics during the shoulder flexion and slouched sitting tasks [A and C]. The other camera was positioned above participant's head (approximately 1 meter) to record trunk rotation (functional task [B]). Anatomic landmarks were identified and marked on each participant by manual palpation: greater tubercule of the humerus on the left side, back of the left hand, acromion on both sides and C7 spinal process. To synchronize EMG and kinematics data, a sound was generated at the beginning and at the end of each functional task and recorded with the 16-bit CED DAQ (sampled at 1000 Hz) and the digital video cameras. This synchronization signal was used to determine when the longissimus pars lumborum turned on/off during the functional tasks and quantify movements globally.

Data Analysis
Experiment 1: The identification of single MUs from the action potentials recorded with the microelectrodes was performed using an algorithm from the Spike2 software (Cambridge Electronic Design) based on their size, shape and timing. The shape and discharge rate of MU action potentials were used to verify manually and include actions potentials that could have been missed by the automated algorithm. This procedure also helped identify action potentials when superimposition with other MUs occurred. MUs with a minimum of 300 action potentials during the lumbar isometric contractions were considered to compute spike-triggered averages in the fine-wire multi-unit EMG (Farina *et al.*, 2008; Héroux *et al.*, 2015). We determined the spatial localization of a single MU by evaluating the fine-wire recording sites where the spike-triggered fine-wire EMG average crossed a threshold

value of ±4 standard deviations (SD) of the baseline activity computed in a 25ms window (-35ms to -10ms) prior the target MU spike time (Héroux *et al.*, 2015; Luu *et al.*, 2018) (Figure 2). MU territories corresponded to the number of consecutive fine-wire recording sites with spike-triggered averages that exceeded the ±4SD threshold. We estimated MU territories for all MUs recorded with the microelectrodes (L1, L2, L3 and L4) for each participant. In a few cases (N=15), spike-triggered averages reached threshold from non-consecutive sites. In these instances, the gap was included in the MU territory when the spike-triggered averages on either side of the gap exceeded the ±4SD threshold. The size of MU territories was estimated based on the distance between insertion sites. As reported previously by Héroux *et al.* (2015), we also identified the same MU from the spike-triggered fine-wire EMG averages when we thought we were recording different single MUs from the microelectrode (at the same or from a different lumbar site). We confirmed these occurrences when the spike-triggered fine-wire EMG averages were identical at all sites (e.g. same template) for (presumed) different microelectrode MUs. When this happened, only one occurrence of the MU was considered for the further analysis. In addition, we estimated the averaged MU discharge frequency (Hz) using the number of motor unit action potentials identified from a single MU in one trial divided by the length of the trial. We removed interspike intervals longer than 500ms (Lothe *et al.*, 2015) to remove periods when the MUs were inactive.

To compare the orientation of the longissimus pars lumborum muscle fibers to previous work (McGill *et al.*, 2000), we quantified their orientation for each participant using ImageJ software (Schneider *et al.*, 2012) from the stitched ultrasound pictures taken at L1, L2, L3 and L4. Muscle fiber orientation was estimated using the angle between the fiber and the skin surface, as previously described (McGill *et al.*, 2000). The orientation of muscle fibers was calculated near the depth of the fine-wire electrode insertion (~2cm). We highlight that ultrasound estimates of pennation angles using this method are typically overestimated (Bolsterlee *et al.*, 2016) but we present pennation angles to allow comparison with previously reported values using the same method (McGill *et al.*, 2000; Harriss & Brown, 2015).

Experiment 2: We estimated the arm and trunk peak angles during the functional tasks using 2D vectors between landmarks created with Kinovea software (Kinovea 0.8.15 for Windows). For the shoulder flexion task, we estimated shoulder flexion using the angle between a horizontal vector (parallel to the ground) and a vector between the greater tubercule of the humerus and the back of the hand. Trunk axial rotation was estimated using a vector between the left acromion and C7 spinal process and a vector corresponding to the neutral seated position using the same landmarks (defined as zero degree for each participant). Only left trunk rotation (ipsilateral contraction) was considered due to the negligible contribution of the left longissimus pars lumborum during right trunk rotation. To quantify muscle activation during the functional tasks, we computed the root mean square (RMS) of the EMG signals from each longissimus pars lumborum level (L1 to L4). First, the EMG signals were digitally band-pass (20-450Hz, 4th order Butterworth filter) and band-stop (2nd order Butterworth filter, 59-61 Hz) filtered. The RMS from each multi-unit EMG was computed using consecutive 500ms windows that overlapped for 250ms. We extracted the minimum RMS value 1s before movement onset (baseline) and 1s at the end of the movement. The minimum RMS was chosen because we expected muscle activity to decrease during the functional tasks for some lumbar regions. The end of the movement for each functional task was determined based on the kinematic data ([A] Shoulder flexion: full flexion of the arm, [B] Trunk rotation: maximum left trunk rotation, and [C] Slouched sitting: maximum slouched posture). Longissimus pars lumborum EMG activity was normalized with respect to the EMG recording during the back isometric extension MVC. Normalized RMS EMG values were obtained by dividing the RMS EMG from each multi-unit recording extracted during the functional tasks by the RMS EMG of the corresponding multi-unit recording obtained during the MVC trial.

[Figure 2]

Statistical Analysis

To determine if the recorded MUs were best represented as a uniform distribution or from multiple distributions, we estimated Gaussian mixture models (GMM) with a linear mixed-effects model (LMM) similar to the methods proposed by Ng and McLachlan (2005). The linear mixed-effects model was added to account for possible subject-specific biases in the distributions of individual MUs. These analyses were performed for one (suggesting the longissimus MU territories are distributed along the entire length of the muscle), two and three distributions (suggesting that longissimus MU territories are spatially organized in two or more main territories). We do not present the results from the three-distribution model because it failed to converge more than half of the time and when it converged, two of the distributions were identical (replicating the results from the two-distribution model). The choice of the mixture model that best fit the distribution of MUs was made according to the Akaike Information Criterion (AIC), with the model having the lowest AIC representing the best candidate model. We then calculated the Aikaike weights $(w_i(AIC))$ for each model using the following equation (Burnham & Anderson, 2002; Wagenmakers & Farrell, 2004):

$$w_i(AIC) = \frac{exp\left[-\frac{1}{2} \times \Delta_i AIC\right]}{\sum_{k=1}^{K} exp\left[-\frac{1}{2} \times \Delta_k AIC\right]}$$

where $\Delta_i(AIC)$ represents the difference between the AIC of the current model to the one of the best candidate model (i.e. lowest AIC) and K=2 representing the one-distribution and two-distribution mixtures models. The ratio of the Aikaike weights ($w_{AIC_{min}}/w_{AIC_{max}}$) can be interpreted as the probability that the model with the lowest AIC (AIC_{min}) represents the data distribution better than the alternate model with largest AIC (AIC_{max}). The MUs belonging to a given distribution were determined based on the 95% confidence intervals (95% CI) from the GMM with LMM; note that half a vertebral level represents for example L2 -> L2/L3. These analyses were performed using Matlab software (2018b version, Mathworks, Natick, MA, USA).

To assess the regional activation of the longissimus for each functional task, we used non-parametric tests because our data were not distributed normally (Kolmogorov–Smirnov).

For the baseline RMS and RMS at the end of the movement, separate Kruskal-Wallis ANOVAs were used to compare RMS EMG activation between longissimus levels for each functional task. When the Kruskal-Wallis test was significant, EMG activation levels between the most rostral and caudal levels (L1 and L4) were compared using a Mann-Whitney test for independent measures. All statistical analyses were performed using Statistica (TIBCO Software version 13.3 Inc, Palo Alto, CA, USA) and statistical significance was set at $p \leq 0.05$.

RESULTS

Experiment 1: Motor unit territory

Across all trials and participants, a total of 207 MUs were recorded from the microelectrodes. After removing MU duplicates recorded in different trials, a total of 73 MUs (6-12 MUs per participant) were further analyzed (Table 1). MU discharge frequency ranged from 5.1 to 8.6 Hz (Table 1). From the 73 MUs, 31 exhibited territories that spanned the rostral sites of the longissimus pars lumborum (L1 to L3) and 22 spanned the caudal sites (L3 to L4). Two MUs spanned all lumbar sites (L1 to L4) whereas twelve had muscle fibers spanning partially the rostral (L1 to L3) and caudal (L3 to L4) territories (Figures 3 and 4A). The descriptive statistics and the MU territories suggest there are two main MU territories within the human longissimus pars lumborum.

These observations were confirmed by the Gaussian mixture model that included a linear mixed-effects model to account for individual motor units being clustered within individuals. The model using two territories exhibited a better fit to the data (AIC = 451.9) than the one using a single territory (AIC = 522.6). Based on the ratio of the Aikaike weights, the model with two MU distributions was 2.25×10^{15} times more probable to explain the data than the one with a single MU distribution. For the principal diagonals of the covariance matrices of the two distributions model, the variance in subject-specific biases was 11 to 10882 times smaller than the total variance on the Gaussian distributions. When removing the subject-specific bias parameters (i.e. Linear Mixed Model), we observed smaller AICs for the one and two GMMs (504.5 and 413.6) because the models

performed as well but with fewer parameters. The centroids of the two distribution model accounting for subject-specific biases were located at L2 (95% CI: ± 0.3 vertebral level) and between L3 and L3-L4 (95% CI: ± 0.6 vertebral level), with the L2 centroid exhibiting a one vertebral level distribution (i.e. L1 to L3 territory) on each side of the centroid (95% CI: ± 0.3 vertebral level) and the L3/L3-L4 centroid showing a 0.5 vertebral level distribution (i.e. ~L3 to L4 territory) on each side of the centroid (95% CI: ± 0.2 vertebral level; Figure 4B). Based on the 95% CI from this two-distribution model, we estimated that 32 MUs exhibited territories that spanned the rostral region, 30 MUs spanned the caudal region and 11 MUs where outside the two main distributions. These results corresponded well to the description of MUs territories based on Figure 4A. Based on the distances between the multi-unit EMG recordings, we estimated the mean size of the rostral MUs territories (L1 to L3) at 5.9cm and the mean size for the caudal (L3 to L4) territory at 3.1cm (Table 2). Muscle fiber orientation measured from the ultrasound images revealed a larger pennation angle for the caudal lumbar levels than the rostral ones (Table 3 Figure 2).

[Tables 1, 2, 3; Figures 3, 4]

Experiment 2: Functional tasks

The activation of longissimus pars lumborum muscle was variable between sites, tasks and participants. However, all participants exhibited regional activation in at least one task (Fig 5). At baseline, RMS EMG did not differ between vertebral levels for all functional tasks (Kruskal-Wallis ANOVAs, all p values ≥ 0.91). All participants were able to complete the full range of motion during the shoulder flexion and trunk rotation tasks, reaching 91 degrees (SD=8) of shoulder flexion and 37 degrees of torso axial rotation (SD=7), respectively. At the end of full shoulder flexion, activation of the longissimus pars lumborum did not differ between vertebral levels across participants (Kruskal-Wallis ANOVA, p=0.80; Figure 5A). At the end of the left trunk rotation, however, participants exhibited a significant difference in longissimus activity between vertebral levels (Kruskal-Wallis ANOVA, p=0.039; Figure 5B). When comparing longissimus activity between the most rostral (L1) and the most caudal (L4) vertebral levels at the end of left trunk rotation,

RMS EMG was 16% higher for the L1 than the L4 level (Mann-Whitney test, p=0.004). Finally, when adopting a slouched sitting position, no statistical difference was observed for the RMS values estimated at the L1 to L4 vertebral levels (Kruskal-Wallis ANOVA, p=0.96).

[Figure 5]

DISCUSSION

We investigated the distribution of MU territories in the longissimus pars lumborum muscle. Based on previous animal studies (Wada *et al.*, 2003; Durbaba *et al.*, 2007) and the anatomy of the human longissimus, we hypothesized that the longissimus pars lumborum MUs would be spatially organized in distinct territories. The results of the current study support our hypothesis, suggesting that longissimus pars lumborum MUs are spatially localized in at least two main territories. Distinct rostral and caudal activation of the longissimus pars lumborum observed only during left trunk rotation further support the presence of regional activation in the longissimus muscle. These results suggest the presence of at least two muscle regions in the longissimus pars lumborum that can be activated preferentially during certain functional tasks.

MUs in the human longissimus pars lumborum have a non-uniform distribution along the length of the muscle. Less than 3% of longissimus pars lumborum single MUs recorded were distributed uniformly along its entire length. Although muscle fibers of a single MU can occupy a defined regions within a muscle (Heckman & Enoka, 2012), this has not been observed in all human muscles. Héroux *et al.* (2015) and Luu *et al.* (2018) showed a mostly uniform distribution of muscle fibres belonging to a MU in the medial gastrocnemius and in the genioglossus, respectively. The defined MU territories we observed in the human longissimus pars lumborum are in line with findings in the cat where stimulation of a nerve branch innervating the longissimus generated a localized action potential spanning mainly adjacent segments (Wada *et al.*, 2003; Durbaba *et al.*, 2007). Moreover, the human longissimus pars lumborum exhibits multiple origins onto the lumbar and lower thoracic

vertebrae, a multi-layered organization of their insertion on the lumbar intermuscular aponeurosis and segmental innervation (Macintosh & Bogduk, 1987; Kalimo *et al.*, 1989; Bogduk & Baker, 2014), providing supporting anatomical evidence for the presence of defined MU territories in that muscle.

During small isometric lumbar extension contraction (mostly <10% MVC), two clear MU distributions were observed in the rostral (L1 to L3) and caudal (L3 to L4) regions of the longissimus muscle. These findings were confirmed by the distributions estimated using the Gaussian mixture model (with linear mixed-model), with the model including two MU distributions being more likely to represent the data than the one including only a single MU distribution. Fine-wire EMG related to all MUs was recorded at the L3 level. Based on the model, approximately 44% (n=32) of the recorded MUs were spatially localized to the rostral region (spanning 4 different recording sites, i.e. 2 vertebral levels corresponding to L1-L3), 41% (n=30) exhibited a spatial distribution localized in the caudal region (spanning two recording sites, i.e. 1 vertebral level corresponding to ~L3-L4) of the longissimus pars lumborum muscle and 15% (n=11) of the recorded MU exhibited territories not limited to the rostral or caudal region. Therefore, we propose that the longissimus pars lumborum exhibits at least two MU territories. The size of the rostral MUs territory (L1 to L3) was almost twice (~ 90%) as long as the caudal territory. The different size between these two MU territories is supported by the regional differences in muscle architecture: smaller muscle fiber angles were observed in the rostral region and thus spanned more lumbar segments.

The presence of two main regions in the left longissimus pars lumborum muscle was also observed during the left trunk rotation task. While distinct activation of longissimus pars lumborum sub-regions was observed in all participants, inter-individual variability in muscle regional activation was observed to execute the same motor tasks. This suggests that although the central nervous system has the means to selectively activate distinct regions of the longissimus pars lumborum muscle based on the task, such regional activation is not consistently observed between individuals for a given task. Example of

selective activation of longissimus pars lumborum sub-regions were observed near the end of trunk axial rotation (~37 degs). On the other hand, a general increase of muscle activity at all lumbar sites was observed for other tasks such as the initiation of shoulder flexion, supporting previous reports (Eriksson Crommert *et al.*, 2015; Takahashi *et al.*, 2015). Altogether, the current findings demonstrate that the longissimus pars lumborum muscle can be recruited as a single entity or based on its rostral and caudal sub-regions. Note that two main regions of activation have also be reported for the longissimus thoracis muscle during axial trunk rotations (Lee *et al.*, 2005). Related to spinal stabilization, our findings further suggest that the longissimus pars lumborum muscle may play a role in regional spinal stabilization instead of stabilizing the whole lumbar region as previously suggested (Bergmark, 1989; Moseley *et al.*, 2002).

A central question in sensorimotor physiology relates to how the central nervous system activates muscles for movement. When executing a motor task, the brain may optimise certain cost functions to determine how motion will be performed (Todorov & Jordan, 2002; Finley *et al.*, 2013). For the activation of muscles, MUs are typically recruited according to Henneman's size principle, i.e. from the smallest to the largest MU (Henneman, 1981). It has also been proposed that MUs can be recruited based on task demands (Loeb, 1985) and their mechanical advantage for the task (neuromechanical principle; Butler & Gandevia, 2008; Hudson *et al.*, 2019). For example, the recruitment of MUs in respiratory muscles will be favoured according to a central mechanism to produce an efficient ventilation of the lungs (mechanical advantage). The neuromechanical principle has also been applied to the psoas major and the quadratus lumborum to explain how the central nervous system could selectively activate different regions of these muscles to adapt to external forces applied to the spine (Park *et al.*, 2014). Based on fiber orientations variation of the erector spinae muscles during functional tasks (Harriss & Brown, 2015), it is tempting to propose that the localized activation of MUs in the longissimus pars lumborum muscle may be associated with their mechanical advantage. Although attractive, this proposal requires extensive anatomical and biomechanical analyses that are outside the scope of the present experiment. Nevertheless, localized activation of sub-regions in the

longissimus pars lumborum adds important anatomical and physiological information that improves our understanding of lumbar muscle activation during motor tasks.

Limitations

A main limitation of the current study is that most MUs were recorded during weak back extension contractions (between 1 and 10% MVC) and less than 25 percent were recorded during moderate contractions (up to 42% MVC). Therefore, it is difficult to draw conclusions regarding MU distribution during high intensity contractions. The presence of "gaps" in MU spike-triggered averages also occurred (dashed lines in Figure 4A). These observations may reflect a level of uncertainty which could lead to a misinterpretation of MU territories and increase the risk of underestimation due to the small recording region of the multi-EMG indwelling electrodes. However, this limitation was previously reported in medial gastrocnemius muscle study and the authors showed that MU territories were not regionally localized (Héroux *et al.*, 2015). Spatially localized muscle activation patterns were observed during trunk rotation, confirming the results from the single MU analyses, but our small sample size requires caution regarding the reproducibility of these findings. Finally, we cannot exclude the possibility of EMG contamination from others lumbar muscles, such as the iliocostalis or the multifidus, but data from a feline model suggests that cross-talk is less than 2.7% for wire recordings in neighbouring muscles (Solomonow *et al.*, 1994).

CONCLUSION

Muscle fibers belonging to the longissimus pars lumborum were mainly organized in two MU territories spanning the rostral (L1-L3) and caudal (L3-L4) regions of the muscle. These two muscle regions could also be activated preferentially during trunk axial rotation. Such segmental organization and voluntary activation of the human longissimus pars lumborum corresponds well with the longissimus motoneurone organization observed in cats. Selective activation of the human longissimus pars lumborum muscle may have important fundamental and clinical implications for movement production and spinal stabilization of the lumbar spine.

REFERENCES

Beretta Piccoli M, Rainoldi A, Heitz C, Wuthrich M, Boccia G, Tomasoni E, Spirolazzi C, Egloff M & Barbero M. (2014). Innervation zone locations in 43 superficial muscles: toward a standardization of electrode positioning. *Muscle & nerve* **49,** 413-421.

Bergmark A. (1989). Stability of the lumbar spine. A study in mechanical engineering. *Acta Orthop Scand Suppl* **230,** 1-54.

Bogduk N. (1983). The innervation of the lumbar spine. *Spine* **8,** 286-293.

Bogduk N & Baker RM. (2014). *Clinical and radiological anatomy of the lumbar spine*. Elsevier, Edinburgh.

Bogduk N, Wilson AS & Tynan W. (1982). The human lumbar dorsal rami. *J Anat* **134,** 383-397.

Bolsterlee B, Gandevia SC & Herbert RD. (2016). Effect of Transducer Orientation on Errors in Ultrasound Image-Based Measurements of Human Medial Gastrocnemius Muscle Fascicle Length and Pennation. *PLoS One* **11,** e0157273.

Burnham KP & Anderson DR. (2002). *Model selection and multimodel inference - 2nd ed. : a practical information-theoretic approach*. Springer-verlag new york Inc., New york, ny.

Butler JE. (2007). Drive to the human respiratory muscles. *Respir Physiol Neurobiol* **159,** 115-126.

Butler JE & Gandevia SC. (2008). The output from human inspiratory motoneurone pools. *J Physiol* **586,** 1257-1264.

Christophy M, Faruk Senan NA, Lotz JC & O'Reilly OM. (2012). A musculoskeletal model for the lumbar spine. *Biomech Model Mechanobiol* **11,** 19-34.

Durbaba R, Taylor A, Ellaway PH & Rawlinson S. (2007). Spinal projection of spindle afferents of the longissimus lumborum muscles of the cat. *The Journal of physiology* **580,** 659-675.

Eriksson Crommert M, Halvorsen K & Ekblom MM. (2015). Trunk Muscle Activation at the Initiation and Braking of Bilateral Shoulder Flexion Movements of Different Amplitudes. *PloS one* **10,** e0141777.

Farina D, Cescon C, Negro F & Enoka RM. (2008). Amplitude cancellation of motor-unit action potentials in the surface electromyogram can be estimated with spike-triggered averaging. *Journal of neurophysiology* **100,** 431-440.

Finley JM, Bastian AJ & Gottschall JS. (2013). Learning to be economical: the energy cost of walking tracks motor adaptation. *J Physiol* **591,** 1081-1095.

Harris AJ, Duxson MJ, Butler JE, Hodges PW, Taylor JL & Gandevia SC. (2005). Muscle fiber and motor unit behavior in the longest human skeletal muscle. *J Neurosci* **25,** 8528-8533.

Harriss AB & Brown SH. (2015). Effects of changes in muscle activation level and spine and hip posture on erector spinae fiber orientation. *Muscle Nerve* **51,** 426-433.

Heckman CJ & Enoka RM. (2012). Motor unit. *Compr Physiol* **2,** 2629-2682.

Henneman E. (1981). Recruitment of motoneurons: The size principle. In motor units types, recruitment, and plasticity in health and disease. *Progress in Clinical Neurophysiology* **9,** 26-60.

Héroux ME, Brown HJ, Inglis JT, Siegmund GP & Blouin JS. (2015). Motor units in the human medial gastrocnemius muscle are not spatially localized or functionally grouped. *J Physiol* **593,** 3711-3726.

Hudson AL, Gandevia SC & Butler JE. (2019). A Principle of Neuromechanical Matching for Motor Unit Recruitment in Human Movement. *Exerc Sport Sci Rev* **47,** 157-168.

Hudson AL, Taylor JL, Gandevia SC & Butler JE. (2009). Coupling between mechanical and neural behaviour in the human first dorsal interosseous muscle. *The Journal of physiology* **587,** 917-925.

Kalimo H, Rantanen J, Viljanen T & Einola S. (1989). Lumbar muscles: structure and function. *Ann Med* **21,** 353-359.

Lee LJ, Coppieters MW & Hodges PW. (2005). Differential activation of the thoracic multifidus and longissimus thoracis during trunk rotation. *Spine* **30,** 870-876.

Loeb GE. (1985). Motoneurone task groups: coping with kinematic heterogeneity. *J Exp Biol* **115,** 137-146.

Lothe LR, Raven TJ & Eken T. (2015). Single-motor-unit discharge characteristics in human lumbar multifidus muscle. *Journal of neurophysiology*, jn 00010 02014.

Luu BL, Muceli S, Saboisky JP, Farina D, Héroux ME, Bilston LE, Gandevia SC & Butler JE. (2018). Motor unit territories in human genioglossus estimated with multichannel intramuscular electrodes. *J Appl Physiol (1985)* **124,** 664-671.

Macintosh JE & Bogduk N. (1987). 1987 Volvo award in basic science. The morphology of the lumbar erector spinae. *Spine (Phila Pa 1976)* **12,** 658-668.

Marsden JF, Farmer SF, Halliday DM, Rosenberg JR & Brown P. (1999). The unilateral and bilateral control of motor unit pairs in the first dorsal interosseous and paraspinal muscles in man. *The Journal of physiology* **521 Pt 2,** 553-564.

McGill SM, Hughson RL & Parks K. (2000). Changes in lumbar lordosis modify the role of the extensor muscles. *Clin Biomech (Bristol, Avon)* **15,** 777-780.

Moseley GL, Hodges PW & Gandevia SC. (2002). Deep and superficial fibers of the lumbar multifidus muscle are differentially active during voluntary arm movements. *Spine (Phila Pa 1976)* **27,** E29-36.

Ng S-K & McLachlan GJ. (2005). Mixture Model-based Statistical Pattern Recognition of Clustered or Longitudinal Data. In *Proceedings of WDIC2005 (APRS Workshop on Digital Image Computing, Brisbane), Griffith University, Southbank, Brisbane Australia*, pp. 139-144.

Park RJ, Tsao H, Cresswell AG & Hodges PW. (2014). Anticipatory postural activity of the deep trunk muscles differs between anatomical regions based on their mechanical advantage. *Neuroscience* **261,** 161-172.

Schneider CA, Rasband WS & Eliceiri KW. (2012). NIH Image to ImageJ: 25 years of image analysis. *Nat Methods* **9,** 671-675.

Shiraishi M, Masuda T, Sadoyama T & Okada M. (1995). Innervation zones in the back muscles investigated by multichannel surface EMG. *Journal of electromyography and kinesiology : official journal of the International Society of Electrophysiological Kinesiology* **5,** 161-167.

Solomonow M, Baratta R, Bernardi M, Zhou B, Lu Y, Zhu M & Acierno S. (1994). Surface and wire EMG crosstalk in neighbouring muscles. *J Electromyogr Kinesiol* **4,** 131-142.

Takahashi K, Yamaji T, Wada N, Shirakura K & Watanabe H. (2015). Trunk kinematics and muscle activities during arm elevation. *Journal of orthopaedic science : official journal of the Japanese Orthopaedic Association* **20,** 624-632.

Todorov E & Jordan MI. (2002). Optimal feedback control as a theory of motor coordination. *Nat Neurosci* **5,** 1226-1235.

Wada N, Takahashi K & Kanda K. (2003). Synaptic inputs from low threshold afferents of trunk muscles to motoneurons innervating the longissimus lumborum muscle in the spinal cat. *Experimental brain research Experimentelle Hirnforschung Experimentation cerebrale* **149,** 487-496.

Wagenmakers E-J & Farrell S. (2004). AIC model selection using Akaike weights. *Psychonomic Bulletin & Review* **11,** 192-196.

Wakeling JM. (2009). The recruitment of different compartments within a muscle depends on the mechanics of the movement. *Biol Lett* **5,** 30-34.

Additional information

Competing interest

The authors have no conflicts of interest to disclose.

Funding

Author contributions

J.A., M.D. and J.S.B. conceived and designed the experiment. J.A., C.K. and J.S.B. undertook the experimental work and analysis. All authors drafted the manuscript or reviewed it critically for important intellectual content. All authors approved the final version of the manuscript and agree to be accountable for all aspects of the work. All persons designated as authors qualify for authorship, and all those who qualify for authorship are listed.

Table 1. Descriptive data of MUs

		S01	S02	S03	S04	S05	S06	S07	S08	All subjects
Number of spikes for all MUs per trial (M ± SD)		492 ± 109	538 ± 95	480 ± 77	571 ± 109	668 ± 128	713 ± 221	568 ± 166	628 ± 161	584 ± 82
L1	MUs (number)	4	3	1	3	3	2	2	2	Total=20
	DF (Hz, M ± SD)	6.1 ± 0.9	7.1 ± 1.1	5.3	5.9 ± 0.5	8.3 ± 1.4	6.7 ± 0.6	5.4 ± 0.5	6.2 ± 0.7	6.4 ± 1.0
L2	MUs (number)	3	3	1	2	2	2	2	2	Total=17
	DF (Hz, M ± SD)	5.8 ± 1.4	6.5 ± 1.0	6.3	6.6 ± 0.9	6.6 ± 0.8	8.6 ± 0.1	5.1 ± 0.6	6.1 ± 0.5	6.5 ± 1.1
L3	MUs (number)	1	2	2	2	3	1	4	3	Total=18
	DF (Hz, M ± SD)	6.4	6.6 ± 0.5	5.7 ± 0.8	6.3 ± 0.6	6.1 ± 0.4	6.5	5.2 ± 1.0	6.4 ± 0.8	6.2 ± 0.5
L4	MUs (number)	2	2	3	3	4	1	1	2	Total=18
	DF (Hz, M ± SD)	6.5 ± 0.9	5.8 ± 0.2	6.1 ± 0.5	6.8 ± 1.0	7.6 ± 1.0	7.4	6.4	7.5 ± 1.0	6.8 ± 0.7
MUs total		10	10	7	10	12	6	9	9	Total=73

MU: Motor unit; M: Mean; SD: Standard deviation; DF: Discharge frequency; S01 to S08: Subject 1 to 8

Table 2. Estimates of MU territory size (cm)

	S01	S02	S03	S04	S05	S06	S07	S08	Mean ± SD
L1 to L3	6	6	5	7	6	6.2	6	5.2	5.9 ± 0.6
L3 to L4	2.9	3	2.5	4	3	3.4	3.2	3.1	3.1 ± 0.4

MU: Motor unit; SD: Standard deviation; S01 to S08: Subject 1 to 8

Table 3. Longissimus muscle fiber angles (degrees)

	S01	S02	S03	S04	S05	S06	S07	S08	Mean ± SD
L1	9	8	9	7	11	9	7	9	8.6 ± 1.3
L2	12	9	10	9	10	9	9	8	9.5 ± 1.2
L3	12	7	10	9	11	9	7	10	9.4 ± 1.8
L4	13	8	12	13	9	9	10	10	10.5 ± 1.9

SD: Standard deviation; S01 to S08: Subject 1 to 8

Figure and legends

Figure 1. The longissimus pars lumborum muscle
A, Anatomy of the longissimus pars lumborum. On the right, the lines indicate muscle and musculotendinous fascicles originating from the different vertebral levels and attaching on the posterior sacrum and medial edge of the iliac crest. B, Ultrasound image showing the insertion of a fine-wire electrode (with the hypodermic needle) into the longissimus pars lumborum at L1.

Figure 2. Procedures and EMG signal processing.
Representative data from a single participant (n=1). Multi-unit fine-wire electrodes (white circles) were inserted in seven location with a depth of 2cm into the longissimus pars lumborum muscle (from L1 to L4) using ultrasound guidance. One microelectrode (white triangle) was inserted as close as possible to the tips of one fine-wire electrode located at L1, L2, L3 (current example) or L4. During a back isometric contraction, the activity of several MUs could be observed on the fine-wire recordings. At the same time the microelectrode recorded single MU discharge activity. The microelectrode signal showed a single MU. When a spike-triggered average exceeded 4 times the baseline activity (grey rectangle), it was considered that the identified MU had muscle fibers in close vicinity to the fine-wire recording electrode (black star). All vertical scale bars are in microvolts.

Figure 3. Distribution of muscle fibers from longissimus pars lumborum MUs.
A, Data from one representative participant (n=1). Spike-triggered averages in the fine-wire EMG based on the firing of a MU recorded at L1 indicate that this MU has a spatial distribution that spans 5 recording sites in red (from L1 to L3). B, Data from another representative participant (n=1). Spike-triggered averages in the fine-wire EMG based on the firing of a MU recorded at L4 indicate that this MU has a spatial distribution that spans 3 recording sites in red (from L3 to L4). The grey area indicates ± 4SD of baseline. Sites

with spike-triggered average having an action potential crossing ± 4SD are indicated by a black star. All vertical scale bars are in microvolts. N indicates the number of spikes for the single MU.

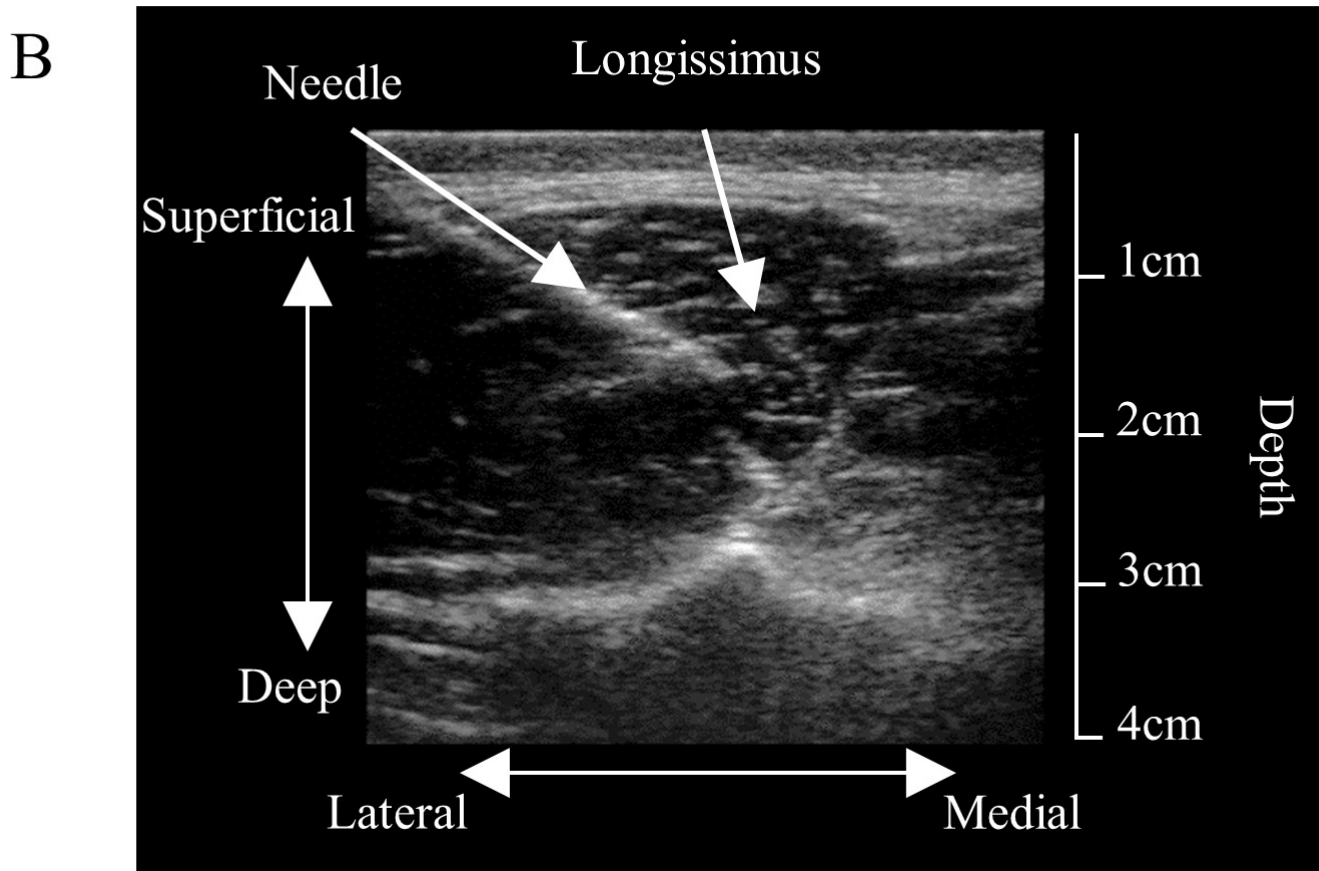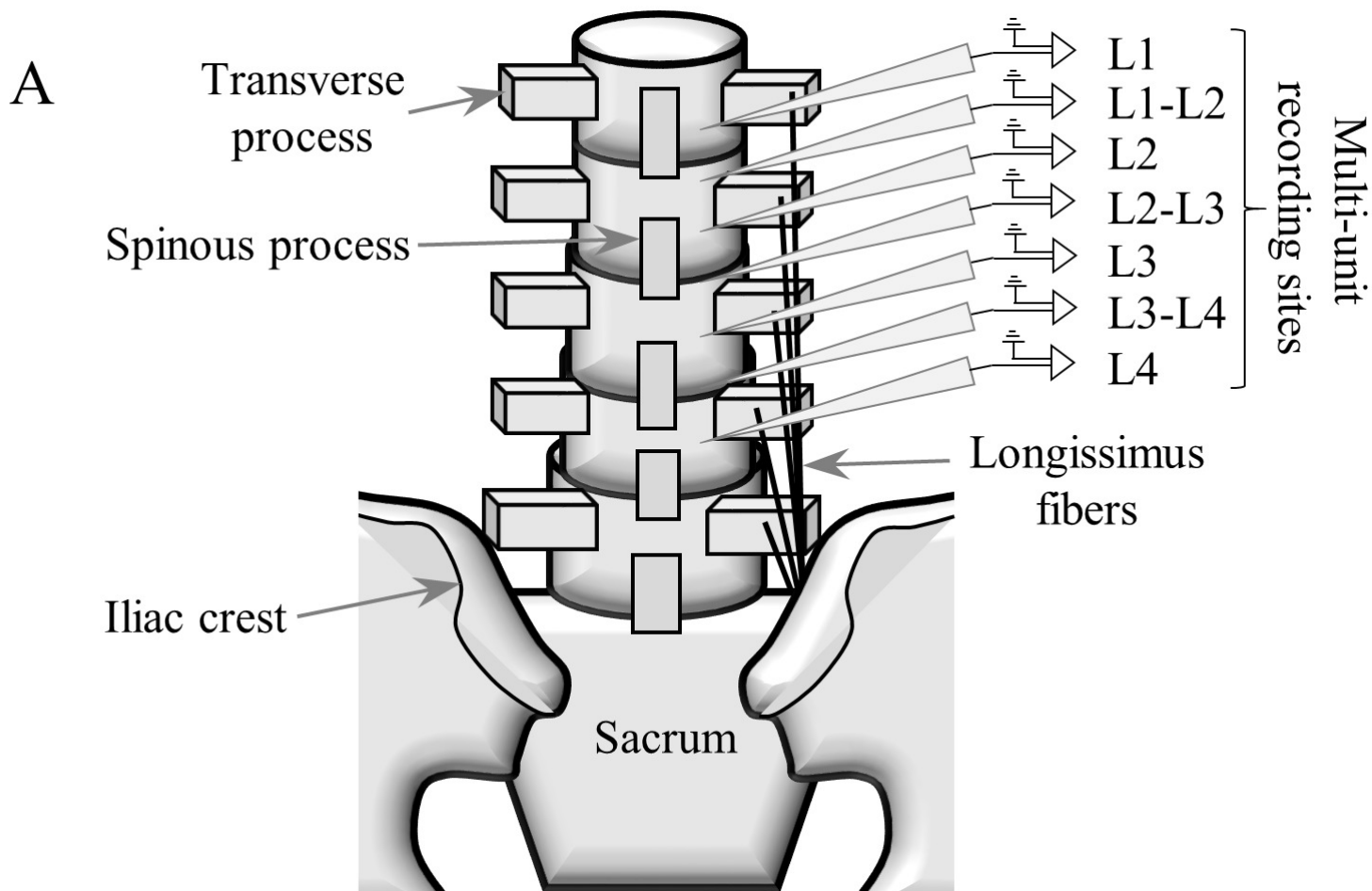**Figure 4. Spatial distribution of the 73 MUs recorded in the longissimus pars lumborum.**

A, Filled circles indicate MUs that were recorded from the microelectrode at a given site (L1, L2, L3 or L4). Vertical lines indicate the spatial distribution of a MU on the spike-triggered averaged traces. Dashed lines indicate MUs that were recorded from the microelectrode at a given site but for which the spike-triggered average in the fine wire EMG exhibited gaps at some sites.
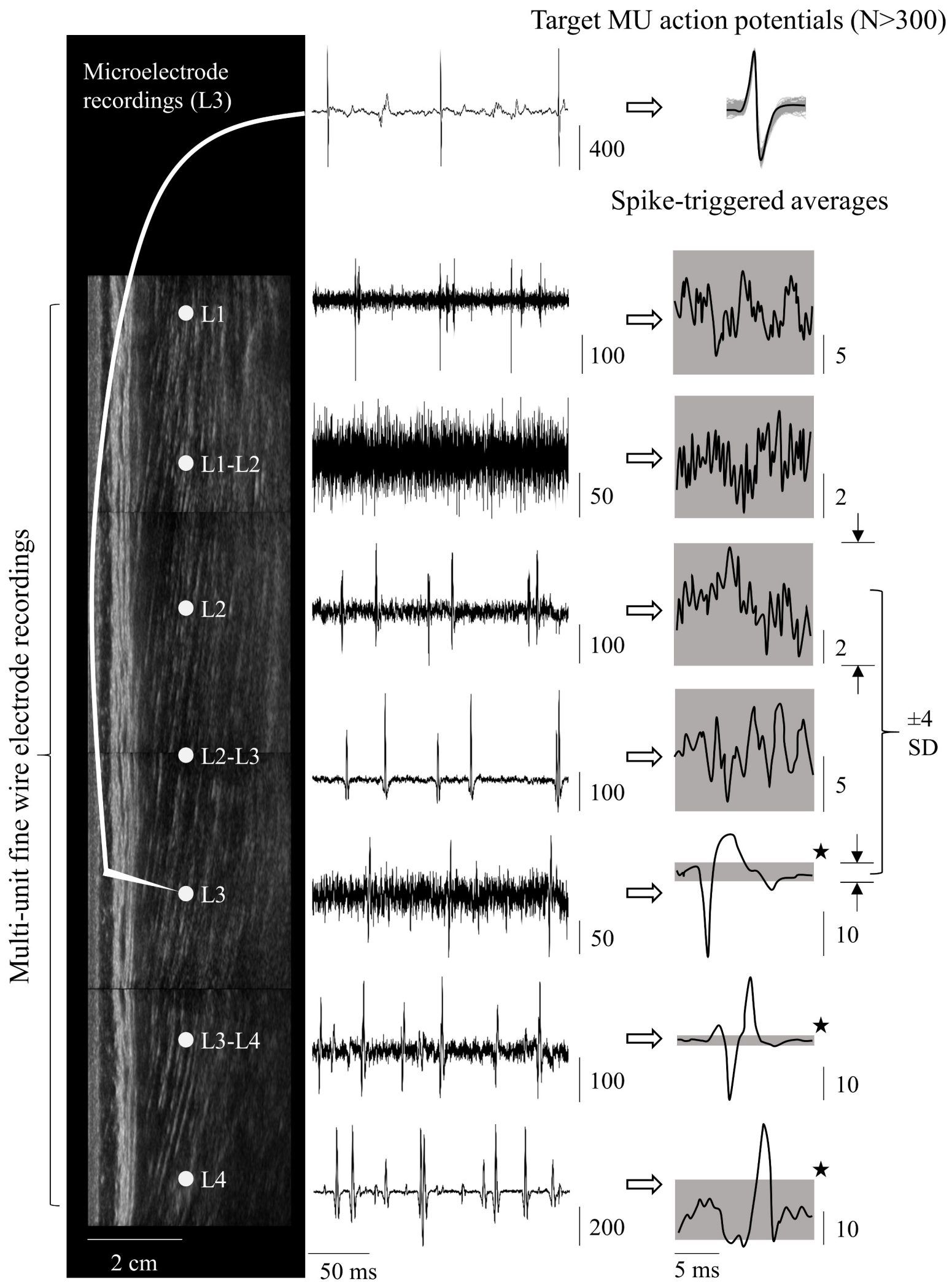
B, Representation of MU distribution based on the Gaussian mixture model (GMM) and linear mixed-effects model (LMM) with two components. The dashed ellipses represent 95% confidence interval for distribution of MUs using two components. The x-axis represents the size of MU territories (in vertebral levels on each site of the centroid) while the y-axis represents the middle localisation of each MU territory. The first territory has a centroid location at ~L2 with a distribution over one vertebral level on each side of the centroid (from L1 to L3). The second territory exhibited a centroid location between L3 and L3-L4 with a distribution over 0.5 vertebral level of each side of the centroid (from ~L3 to L4). The dots representing the MUs vary in size according to the number of MUs on a specified x,y location. The localisation of each dot is based on the spatial distribution of each MU per participant. Inside each dot, individual participants are represented with different colors.

Figure 5. Spatial distribution of muscle activity during the functional tasks.

A, Representative data from a single participant (n=1) during the shoulder flexion task. Note the sustained muscle activity of the longissimus pars lumborum only from L3 to L4 levels and nearly absent activity from L1 to L2-L3 while holding a complete shoulder flexion. B, Representative data from a single participant (n=1) during the trunk rotation

task. Note the sustained muscle activity of the longissimus pars lumborum from L1 to L3 levels with minimal activity at the L3-L4 level during the left trunk rotation. In both figures, the dashed rectangles represent the time-window considered for the RMS computation. All vertical scale bars are in microvolts.

A

Transverse process

Spinous process

Iliac crest

Sacrum

Longissimus fibers

L1
L1-L2
L2
L2-L3
L3
L3-L4
L4

Multi-unit recording sites

B

Needle

Longissimus

Superficial

Deep

1cm
2cm
3cm
4cm

Depth

Lateral

Medial

Microelectrode recordings (L3)

Target MU action potentials (N>300)

400

Spike-triggered averages

Multi-unit fine wire electrode recordings

L1

100

5

L1-L2

50

2

L2

100

2

±4 SD

L2-L3

100

5

L3

50

★

10

L3-L4

100

★

10

L4

200

★
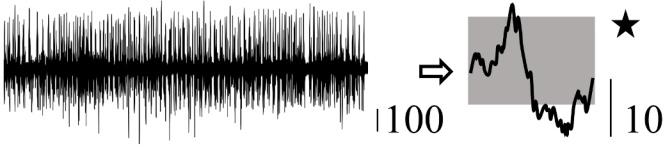
10

2 cm

50 ms

5 ms

A

Microelectrode single motor unit recordings L1 (N=572)

Multi-unit fine-wire electrode recordings   Spike-trigger averages

L1

L1-L2

L2

L2-L3

L3

L3-L4

L4

B

Microelectrode single motor unit recordings L4 (N=815)

Multi-unit fine-wire electrode recordings   Spike-trigger averages

A

L1 | 100
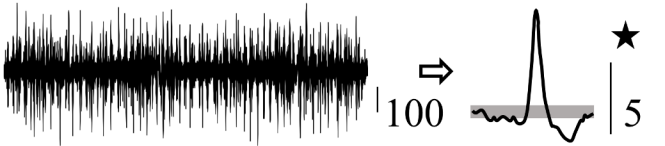L1-L2 | 100
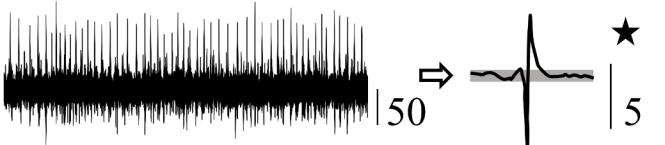L2 | 100
L2-L3 | 100
L3 | 100
L3-L4 | 100
L4 | 100

1 sec

B

L1 | 200
L1-L2 | 100
L2 | 100
L2-L3 | 100
L3 | 100
L3-L4 | 100
L4 | 100

1 sec